

Near-Field Optical Characterization of Nanocomposite Materials

Lukas Novotny

The Institute of Optics, University of Rochester, Rochester, New York 14627

We present a near-field optical technique which makes use of the strongly enhanced optical field at a laser-illuminated metal tip. The enhanced field is used to locally excite the sample under investigation by multiphoton absorption. An optical scan image with spatial resolutions down to 20 nm is established by detecting the emitted fluorescence. The principle of the method is described and experimental results are demonstrated for samples of J-aggregates of PIC dye molecules. Ongoing experiments on nanocomposite, Er^{3+} -doped oxyfluoride glass-ceramics are discussed.

I. Introduction

NANOCOMPOSITE materials consist of nanoscale constituents which exhibit optical and electronic properties that differ from the corresponding macroscopic properties. There is a wide range of potential applications of nanocomposite materials. Among them are electrical and optical sensors, dispersions, coatings, and novel optical glasses. While there is a strong effort in the synthesis of nanostructures and nanocomposite materials, there is also a need to develop suitable techniques to probe the physical properties of these novel materials. In fact, the recent rapid advances in nanotechnology are due in large part to our newly acquired ability to measure and manipulate individual structures on the nanoscale. Among these techniques are scanning probe microscopes, optical tweezers, high-resolution electron microscopes, and others.

Currently, there is a big effort to understand the physical and chemical properties of nanoscale systems. In the bottom-up approach one first intends to understand the building blocks on a nanometer scale before assembling them into a functional device. However, the properties of the building blocks can change once they are embedded into a macroscopic structure. This change is due to interactions between the building blocks and also interactions with the environment. In fact, one of the most interesting aspects of materials at the nanoscale involves properties dominated by collective phenomena. In some case, collective phenomena can bring about a large response to a small stimulus. To investigate such phenomena it is necessary to study the properties of single nanostructures in a complex environment. However, this requires instrumentation with high spatial resolution.

In this paper we describe a near-field optical technique for the characterization of nanocomposite materials. Using this technique, spectroscopic measurements with spatial resolutions of 20 nm have been demonstrated.¹ Here, we will first present experimental results for samples of J-aggregates of PIC dye molecules. These results demonstrate the principle and the capabilities of this near-field optical technique. We then discuss our current experiments on nanocomposite oxyfluoride glass-ceramics.²

II. Near-Field Optical Microscopy and Spectroscopy with Laser-Illuminated Metal Tips

Optical spectroscopy provides a wealth of information on structural and dynamical properties of materials. Combining optical spectroscopy with microscopy is especially desirable because the spectral features can be spatially resolved. In recent years a novel microscopy, called near-field optical microscopy,³ has extended the range of optical measurements beyond the diffraction limit and stimulated interests in many disciplines, especially material sciences and biological sciences.⁴ In the most widely adapted aperture approach,⁵ light is sent down an aluminum-coated fiber tip of which the foremost end is left uncoated to form a small aperture. Unfortunately, only a tiny fraction of the light coupled into the fiber is emitted through the aperture because of the cutoff of propagation of the waveguide modes. The low light throughput and the finite skin depth of the metal are the limiting factors for resolution. Nowadays, it is doubted that an artifact-free resolution of 50 nm will be surpassed by the aperture technique. However, many applications in nanotechnology require higher spatial resolutions.

To overcome this limitation, we introduced a new apertureless technique.⁶ It makes use of the strongly enhanced electric field close to a sharply pointed metal tip under laser illumination. Depending on the tip material and the polarization of the excitation, the energy density close to the metal tip can be 2 to 3 orders of magnitude larger than the energy density of the illuminating laser light. The field enhancement arises from a high surface charge density at the tip induced by the incident light polarized along the tip axis. In contrast, incident light with polarization perpendicular to the tip axis results in no field enhancement. Figure 1 shows the calculated field distribution and induced surface charge density when the gold tip is illuminated with the polarization along the tip axis. Notice that the field enhancement is *not* based on a surface plasmon resonance condition. Instead, it is generated by the quasi-electrostatic singularity at the tip (lightning rod effect).

The principle of the experimental setup is shown in Fig. 2. A laser beam is focused by a high numerical aperture objective onto the sample surface and the tip is laterally positioned into the focal spot. The laser wavelength and polarization are optimized to maximize the field enhancement at the metal tip. The enhanced fields near the tip form a local excitation source which allows for a highly confined optical interaction with the sample surface. This interaction gives rise to a spectroscopic response which is collected by the same objective lens and directed onto a confocal pinhole and a subsequent optical detector. To establish an optical image of the sample surface, the sample is laterally raster scanned while assigning to each point on the sample surface a corresponding spectroscopic signature. The metal tip is maintained within 0.5–2 nm above the sample surface by using a tuning-fork feedback mechanism.⁷ A highly sensitive preamplification allows us to keep the interaction forces between tip and sample in the range of 10–100 pN. Forces in this range do not damage the soft metal tips. A phase-sensitive detection scheme⁸ with a fast time response has been developed to circumvent the limitations imposed by the high Q factor (1600) of the tuning fork resonance. The vertical noise (electrical and mechanical) of the entire system is less than 0.1 nm (rms).

R. K. Brow—contributing editor

Manuscript No. 187937. Received February 15, 2001; approved August 15, 2001. Presented at the Fall Meeting of the Glass and Optical Materials Division, Oct. 1–4, 2000, Corning, NY.
This work was supported by the NSF Grant No. DMR-0078939.

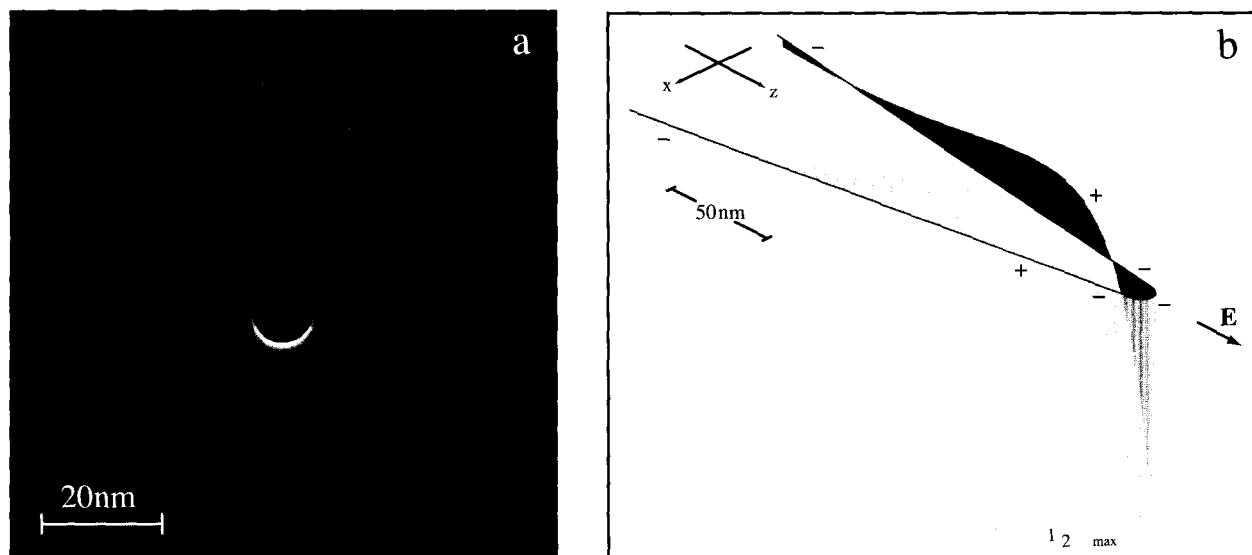


Fig. 1. (a) Calculated field distribution (E^2) near a gold tip illuminated by a plane wave polarized along the tip axis. The electric field is considerably enhanced beneath the tip. (b) Induced surface charge density. The surface charges form an oscillating standing wave. The large surface charge accumulation at the foremost part is responsible for the field enhancement. From Ref. 9.

The direct illumination of the sample surface gives rise to a far-field background signal. If we consider an optical interaction that is based on an n th-order nonlinear process and assume that only the sample surface is active, then the far-field background will be proportional to

$$S_{ff} \sim AI_0^n \quad (1)$$

where A is the illuminated surface area and I_0 is the laser intensity. The signal that we wish to detect and investigate (near-field signal) is excited by the enhanced field at the tip. If we designate the enhancement factor for the electric field intensity by f , then the near-field signal of interest is proportional to

$$S_{nf} \sim a(fI_0)^n \quad (2)$$

where a is a reduced area given by the tip size. If we require that the signal be stronger than the background ($S_{nf}/S_{ff} > 1$) and use

realistic numbers for the areas ($a = (10 \text{ nm})^2$, $A = (500 \text{ nm})^2$), then we find that an enhancement factor of

$$f > \sqrt[n]{2500} \quad (3)$$

is required. For a first-order process ($n = 1$) such as scattering or fluorescence an enhancement factor of 3 to 4 orders of magnitude is required, which is beyond the calculated values. Therefore, the scheme is not applicable to first-order processes and it is necessary to involve higher-order nonlinear processes. For a second-order nonlinear process the required enhancement factor is only 50. This is the reason that our first experiments have been performed with two-photon excitation. Since the enhanced field is highly localized at the end of the tip, the achievable resolution is on the order of the tip diameter. Previous experiments with ultrasharp gold tips produced by focused ion beam milling demonstrated spectroscopic measurements with spatial resolutions on the order of 20 nm.⁹ To date, this is the highest reported spatial resolution of a spectroscopic optical measurement.

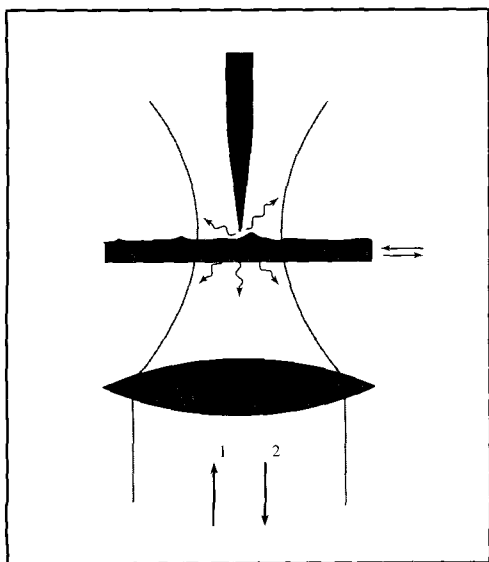


Fig. 2. Principle of the near-field optical technique. A laser beam is focused on a sample surface and a sharply pointed metal tip is held in close proximity above the surface. The enhanced fields at the tip locally interact with the sample surface, thereby exciting a spectroscopic response that is detected by the same objective and directed onto a detector.

III. Experiments on J-Aggregates Using Two-Photon Excitation

The enhanced field at the tip can be established only if the exciting laser light has an electric field component along the tip axis. Therefore, in an on-axis illumination as shown in Fig. 2 one would not expect a strong field enhancement. However, this is true only for a focused beam in the paraxial (weakly focused) approximation. For a beam focused by a lens with a high numerical aperture (NA) an appreciable longitudinal field is built up in the focus of the beam.¹⁰ The longitudinal field is zero on the optical axis. In the focal plane it forms two distinct lobes aligned in the direction of the beam polarization. The strength of this longitudinal field increases with increasing NA of the focusing lens. For a strongly focused beam as encountered in our setup, the longitudinal field strength is only a factor of 5 weaker than the transverse field strength (cf. Fig. 3(c)). An image of the two longitudinal field lobes is shown in Fig. 3(a). To record these images we made use of the fact that the field enhancement is accompanied by increased second-harmonic generation at the metal tip surface. The light of a mode-locked titanium-sapphire (Ti:S) laser ($\lambda = 830 \text{ nm}$) generating $\approx 150 \text{ fs}$ laser pulses has been focused by an NA = 1.4 objective lens on the surface of a bare glass surface and a sharp gold tip was scanned line by line through the focus. An image was

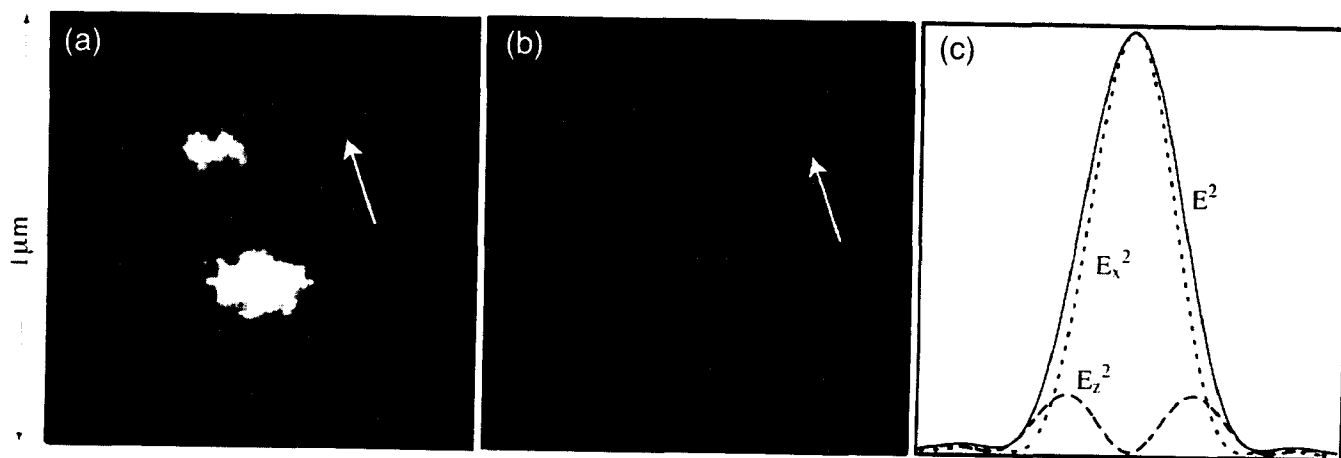


Fig. 3. Longitudinal field lobes in the focal plane of a strongly focused laser beam. The experimental image (a) has been measured by raster scanning the gold tip through the focal plane of the laser beam and recording the second-harmonic light generated at the surface of the tip. The two lobes are aligned in the direction of the laser polarization in agreement with the calculated pattern (b). The arrows indicate the direction of polarization. (c) Longitudinal field strength (E_z^2), transverse field strength (E_x^2), and total field strength (E^2) as a function of the radial coordinate in the focal plane.

generated by recording the intensity of the generated second-harmonic light for each tip position. Figure 3(b) shows that the obtained image is in agreement with the calculated pattern. If the polarization of the laser beam is rotated by 90° , the two lobes rotate as well. Figure 3(c) depicts the longitudinal (E_z^2) and transverse (E_x^2) field strength as a function of the radial coordinate (along the polarization direction) in the focal plane.

To demonstrate the imaging properties of the field enhancement technique we chose a sample which simultaneously generates a near-field and a far-field image. This sample consists of single nanoscale PVS (poly(vinyl sulfate)) strands with J-aggregates of PIC (pseudocyanine) dye.¹¹ The gold tip has been positioned above a longitudinal field lobe in the laser focus and the sample with a single strand of J-aggregates was laterally scanned as schematically shown in Fig. 2. Both the focused Ti:S laser light

and the enhanced field at the gold tip excite the J-aggregates by two-photon absorption. The emitted fluorescence is detected and used to establish an optical raster-scan image. Figure 4(a) shows the topographic (surface profile) image of a single strand of J-aggregates, and Fig. 4(b) shows the simultaneously recorded fluorescence image. The curves beneath the images show an arbitrary cross section. The size of the J-aggregate strand was chosen such that two distinct features can be recognized in the fluorescence image: (1) a broader shoulder due to fluorescence excited by the focused laser light and (2) a sharp peak which corresponds to the fluorescence excited by the enhanced field at the gold tip. Thus, the optical image is a superposition of a far-field image and a near-field image. The near-field peak disappears if the tip is retracted from the sample surface during the imaging process, but the far-field shoulder remains unaffected. Figure 4(c) shows

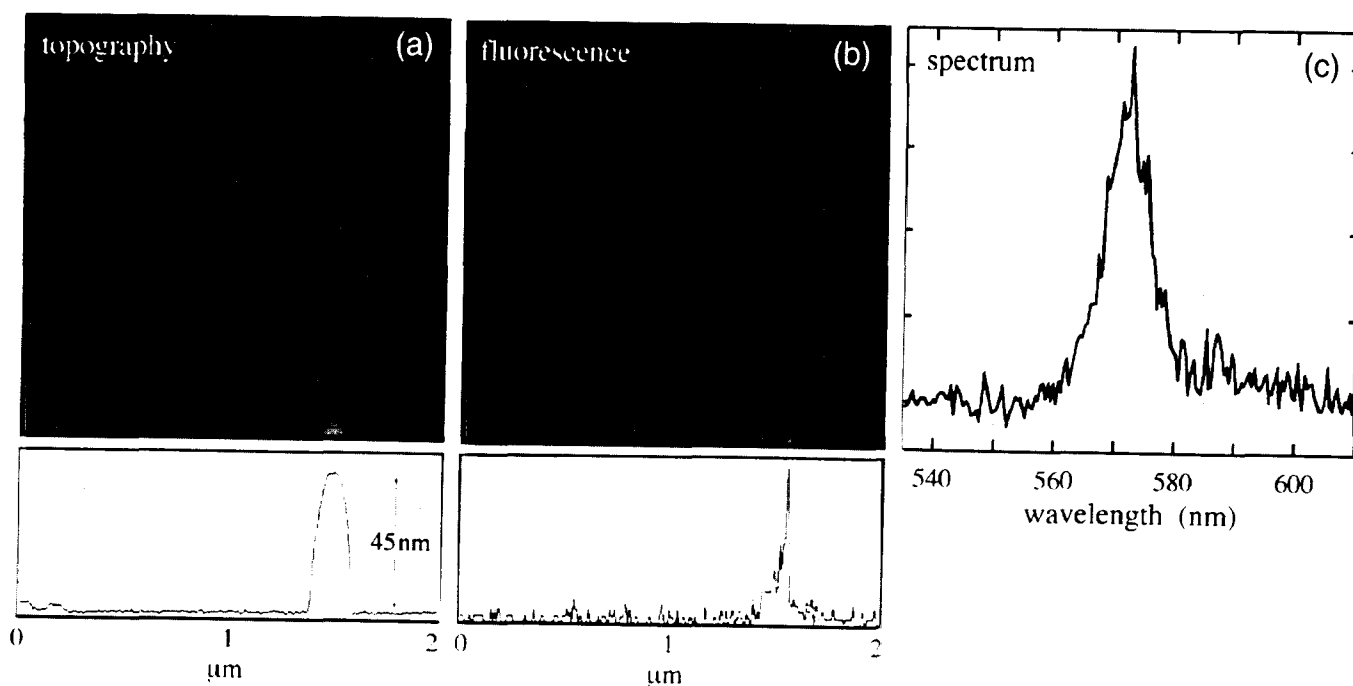


Fig. 4. Simultaneously recorded near-field and farfield image of a single PVC strand with J-aggregates of PIC dye: (a) topographic image; (b) two-photon excited fluorescence image. The sharp peak in the cross section is generated by the enhanced field at the laser illuminated tip (near-field image), whereas the broader Gaussian curve is generated directly by the focused laser light (far-field image). The near-field image is displaced from the center of the beam because of the off-axis location of the longitudinal field lobes (cf. Fig. 3(c)). (c) Spectrum of the emitted fluorescence.

the spectrum of the emitted fluorescence as determined by the PIC dye molecules. If the tip is retracted, the intensity of the spectrum drops because the near-field signal is lost. It can be clearly recognized that the near-field generated vertical line in Fig. 4(b) is slightly displaced from the center of the far-field image. The reason for this displacement is the off-axis location of the longitudinal field lobes. While the far-field image is generated by the total field strength (E^2 in Fig. 3(c)), the near-field image is excited by one of the two longitudinal field lobes (E_z^2 in Fig. 3(c)). Notice that only the surface of the J-aggregate strand contributes to the near-field signal. On the other hand, the entire thickness of the strand determines the strength of the far-field signal. Therefore, by imaging smaller strands it is possible to completely reject the far-field contribution.¹²

IV. Experiments on Nanocomposite Materials

While previous investigations on J-aggregates provided a good understanding and quantification of the field enhancement effect, our current research is focused on nanocomposite materials. One of the systems studied is rare-earth (RE) doped transparent oxyfluoride glass ceramics. These samples consist of a glass matrix with embedded LaF_3 nanocrystallites.¹³ Because the phonon energy in LaF_3 is roughly a factor of 3 lower than in glass, phonon quenching of excited RE ions is smaller inside LaF_3 nanocrystallites than in the glass matrix. Therefore, the lifetime of excited RE ions inside LaF_3 nanocrystallites is higher than in the glass matrix and the stimulated emission cross section is increased. Thus, the optical properties of RE-doped oxyfluoride glass ceramics are controlled by the nanoscale fluoride crystal hosts, whereas the mechanical properties and the durability are determined by the oxide glass. Oxyfluoride glass ceramics are promising materials for fiber amplifiers and up-conversion devices.¹⁴

Our experiments are aimed at optically resolving individual LaF_3 nanocrystallites on the surface of a thin Er^{3+} -doped oxyfluoride glass ceramic sample. The erbium ions are excited from the $^4I_{15/2}$ state by the simultaneous absorption of two photons at $\lambda \approx 850$ nm. This excitation scheme depends quadratically on the excitation intensity and therefore provides good suppression of the far-field background signal. The intermediate virtual level has to be sufficiently separated from the excited levels $^4I_{9/2}$ and $^4I_{11/2}$ to avoid excitation by excited-state absorption and excited-state energy transfer between individual ions. Photons at $\lambda = 550$ nm generated by spontaneous emission from the $^4S_{3/2}$ state are detected to image and optically characterize the sample. The excited-state lifetimes of Er^{3+} are determined by time-correlated photon counting. With our ongoing experiments we are investigating the following: (1) Er^{3+} concentrations in LaF_3 nanocrystallites compared with concentrations in the glass matrix, (2) the homogeneity of Er^{3+} dopants in the sample, (3) the excited-state lifetimes of Er^{3+} in individual LaF_3 nanocrystallites and in the glass matrix, and (4) spectral differences of Er^{3+} emission and absorption due to interactions with the local environment.

The separation between individual LaF_3 nanocrystallites is typically 30–60 nm as determined by atomic-force microscopy.¹⁵ This is an ideal size range for the here-described near-field optical

technique. It is important to use very thin samples and a confocal detection scheme to reduce the far-field background signal. To increase the signal-to-noise ratio it is also possible to apply a three-photon excitation scheme with excitation pulses at $\lambda \approx 1.25$ μm . The signal-to-noise ratio can be further increased by illuminating the metal tip with a higher-order laser mode having a longitudinal field at its focus.¹⁶ A convenient conversion scheme to produce such modes has been developed recently.¹⁷

V. Conclusions

We have described a near-field optical technique with optical spatial resolution down to 20 nm. This method is based on the field enhancement effect at laser-illuminated metal tips. Initial experiments on J-aggregates of PIC molecules demonstrate the principle of the technique. Ongoing experiments on nanocomposite glass ceramics are aimed at optically resolving individual LaF_3 nanocrystallites and measuring the concentration and lifetimes of Er^{3+} dopants.

Acknowledgments

I thank Professor S. Houde-Walter and G. Jones for prompting the experiments on oxyfluoride glass ceramics, and M. Dejneka for providing the samples.

References

1. E. J. Sanchez, L. Novotny, and X. S. Xie, "Near-Field Fluorescence Microscopy Based on Two-Photon Excitation with Metal Tips," *Phys. Rev. Lett.*, **82**, 4014–17 (1999).
2. L. Novotny, E. J. Sanchez, and X. S. Xie, "Near-Field Optical Spectroscopy Based on the Field Enhancement at Laser Illuminated Metal Tips," *Opt. Photonics News*, **10** [12] 24 (1999).
3. "Progress Made in Near-Field Imaging with Light from a Sharp Tip," *Phys. Today*, [July] 18–20 (1999).
4. M. J. Dejneka, "Transparent Oxyfluoride Glass Ceramics," *MRS Bull.*, [November] 57–62 (1998).
5. D. W. Pohl, W. Denk, and M. Lanz, "Optical Stethoscopy: Image Recording with Resolution $\lambda/20$," *Appl. Phys. Lett.*, **44**, 651–653 (1984).
6. A. Lewis, M. Isaacson, A. Harootunian, and A. Muray, "Development of a 500 Å Resolution Light Microscope," *Ultramicroscopy*, **13**, 227–31 (1984).
7. For a recent review, see: B. Dunn, "Near-Field Scanning Optical Microscopy," *Chem. Rev.*, **99**, 2891–928 (1999).
8. E. Betzig and J. K. Trautman, "Near-Field Optics: Microscopy, Spectroscopy, and Surface Modification beyond the Diffraction Limit," *Science*, **257**, 189–95 (1992).
9. L. Novotny, R. X. Bian, and X. S. Xie, "Theory of Nanometric Optical Tweezers," *Phys. Rev. Lett.*, **79**, 645–48 (1997).
10. L. Novotny, E. J. Sanchez, and X. S. Xie, "Near-Field Optical Imaging Using Metal Tips Illuminated by Higher-Order Hermite-Gaussian Beams," *Ultramicroscopy*, **71**, 21–29 (1998).
11. K. Karrai and R. D. Grober, "Piezoelectric Tip-Sample Distance Control for Near Field Optical Microscopes," *Appl. Phys. Lett.*, **66**, 1842–44 (1995).
12. A. G. T. Ruiter, K. O. van der Werf, J. A. Veerman, M. F. Garcia-Parajo, W. H. J. Rensen, and N. F. van Hulst, "Tuning Fork Shear-Force Feedback," *Ultramicroscopy*, **71**, 149–57 (1998).
13. B. Richards, and E. Wolf, "Electromagnetic Diffraction in Optical Systems. II. Structure of the Image Field in an Aplanatic System," *Proc. R. Soc. London, A*, **253**, 358–79 (1959).
14. D. A. Higgins, J. Kerimo, D. A. Vanden Bout, and P. F. Barbara, "A Molecular Yarn: Near-Field Optical Studies of Self-Assembled, Flexible, Fluorescent Fibers," *J. Am. Chem. Soc.*, **118**, 4049–58 (1996).
15. K. S. Youngworth and T. G. Brown, "Focusing of High Numerical Aperture Cylindrical-Vector Beams," *Opt. Express*, **7**, 77–87 (2000). □

A vertical bar on the left side of the page, consisting of a series of colored squares (yellow, orange, red) and a small red diamond at the top.

COPYRIGHT INFORMATION

TITLE: Near-field optical characterization of nanocomposite materials

SOURCE: Journal of the American Ceramic Society 85 no5 May 2002

WN: 0212102109005

(C) Copyright by the American Ceramic Society. All rights reserved.
.ISN:0002-7820..SCJ:y..FTP:y

Copyright 1982-2002 The H.W. Wilson Company. All rights reserved.